

HIPK2 is a potential predictive marker of a favorable response for adjuvant chemotherapy in stage II colorectal cancer

ALESSANDRA VERDINA¹, MICOL DI SEGNI^{1,2}, CARLA AZZURRA AMOREO³, ISABELLA SPERDUTI⁴, SIMONETTA BUGLIONI³, MARCELLA MOTTOLESE³, GIULIANA DI ROCCO^{1*} and SILVIA SODDU^{1*}

¹Unit of Cellular Networks and Molecular Therapeutic Targets, IRCCS Regina Elena National Cancer Institute, I-00144 Rome;

²Department of Sciences, University Roma Tre, I-00146 Rome; ³Pathology Division; ⁴Clinical Trial Center, Biostatistics and Bioinformatic Unit, IRCCS Regina Elena National Cancer Institute, I-00144 Rome, Italy

Received July 22, 2020; Accepted October 23, 2020

DOI: 10.3892/or.2020.7912

Abstract. Colorectal cancer (CRC) is the third most frequently diagnosed type of cancer worldwide. Stage II CRC accounts for ~25% all CRC cases and their management after surgical resection remains a clinical dilemma due to the lack of reliable criteria for identifying patients who may benefit from adjuvant chemotherapy. Homeodomain-interacting protein kinase 2 (HIPK2), a multifunctional kinase involved in numerous signaling pathways, serves several key roles in cell response to different types of stresses, including chemotherapy-induced genotoxic damage. In the present study, immunohistochemistry was performed for HIPK2 on a tissue microarray of primary human tumor samples from 84 patients with stage II CRC, treated (30 patients) or not treated (54 patients) with adjuvant chemotherapy, and sequenced for the *TP53* gene, a key HIPK2 target in genotoxic damage response. It was observed that, regardless of the *TP53* gene status, a high percentage of HIPK2⁺ cells was associated with therapeutic vulnerability in stage II CRC, suggesting a contribution of HIPK2 to drug-response *in vivo*. For the *in vitro* characterization, HIPK2 was depleted in human CRC cells by CRISPR/Cas9 or RNA interference. HIPK2-proficient and HIPK2-defective cells were evaluated for their response

to 5-fluorouracil (5-FU) and oxaliplatin (OXA). The results revealed that HIPK2 depletion induced resistance to 5-FU and OXA, and that this resistance was not overcome by brusatol, an inhibitor of the antioxidant response regulator nuclear factor erythroid 2-related factor 2 (NRF2), which is frequently overexpressed in CRC. By contrast, cell sensitivity to 5-FU and OXA was further induced by brusatol supplementation in HIPK2-proficient cells, further supporting the contribution of HIPK2 in chemotherapy response. Overall, the present results suggested that HIPK2 may be a potential predictive marker for adjuvant-treated stage II CRC and for prospective therapy with NRF2 modulators.

Introduction

Colorectal cancer (CRC) is the third most frequently diagnosed type of cancer (38.7 per 100,000 individuals between 2012 and 2016 in the USA), causing more than half a million deaths per year (1). Stage II CRC is an early-stage in which the tumor has not yet spread to lymph nodes or distant sites, and that has a low risk of recurrence (2). Stage II CRC is a heterogeneous disease both clinically and biologically and, in view of this heterogeneity, the benefits of adjuvant chemotherapy after complete surgical resection vary widely depending on histopathological and molecular tumor features (3). Despite multiple clinical trials and meta-analyses (4), adjuvant chemotherapy in stage II CRC remains an area of great controversy. To date, identifying patients who may benefit from adjuvant therapy is difficult. The decision is mainly based on the presence or absence of high-risk features, such as poorly differentiated histology, the presence of lymphovascular and/or perineural invasion, resection of <12 lymph nodes, bowel obstruction, local perforation or positive margins (5). Consensus Molecular Subtypes of CRC have been proposed based on genome-scale analyses (6), but CRC cases carrying common driver events can vary markedly in their biology (7). Nevertheless, at the biological level, stage II CRC represents a valuable *in vivo* model for studying the effect of chemotherapy on comparable cohorts of patients treated or not treated with chemotherapy.

Homeodomain-interacting protein kinase 2 (HIPK2) is a tyrosine-regulated serine/threonine kinase that modulates different cellular processes, including p53-dependent and -independent

Correspondence to: Dr Silvia Soddu, Unit of Cellular Networks and Molecular Therapeutic Targets, IRCCS Regina Elena National Cancer Institute, Via Elio Chianesi 53, I-00144 Rome, Italy
E-mail: silvia.soddu@ifso.gov.it

*Contributed equally

Abbreviations: CRC, colorectal cancer; HIPK2, homeodomain-interacting protein kinase 2; 5-FU, 5-fluorouracil; OXA, oxaliplatin; NRF2, nuclear factor erythroid 2-related factor 2; TMA, tissue microarray; IHC, immunohistochemistry; moAb, monoclonal antibody; NGS, next generation sequencing; DFS, disease-free survival; SE, standard error; XTT, 2,3-bis-(2-methoxy-4-nitro-5-sulphophenyl)-2H-tetrazolium-5-carboxanilide

Key words: HIPK2, NRF2, brusatol, CRC, adjuvant therapy

apoptosis, differentiation and development (8-11). HIPK2 has long been considered as an oncosuppressor that serves a critical role in cell-fate determination during development and in the response to different genotoxic stresses, such as UV, ionizing radiation and treatment with chemotherapeutic drugs (12-15). Consistent with this hypothesis, low HIPK2 expression has been observed in several types of tumor, including thyroid, bladder, breast, ovarian and esophageal cancer (16-19). As a proof of principle, HIPK2-knockdown impairs p53-dependent and -independent response to therapies, and induces chemoresistance, angiogenesis and tumorigenicity in hepatocellular carcinoma (20), whereas HIPK2 overexpression promotes cell cycle arrest and/or apoptosis, counteracts hypoxia, inhibits angiogenesis and induces chemosensitivity in esophageal squamous cell carcinoma and CRC (10,19,21-23). Conversely, other studies have revealed increased HIPK2 expression and its association with tumor progression in tumor samples from patients with pilocytic astrocytoma, aggressive meningioma, prostate, cervical and colorectal cancer (21,24-27). The aforementioned data suggest that HIPK2 may behave differently depending on the cell context or the tumor histotype; however, the molecular mechanisms need to be defined. Additionally, the HIPK2 protein can undergo post-translational modifications according to its redox state, changing its activity (28). The recently identified crosstalk between HIPK2 and nuclear factor erythroid 2-related factor 2 (NRF2), a master regulator of the antioxidant response considered a 'double-faced' molecule, revealed for the first time HIPK2 regulation at the mRNA level (29), and suggested unexpected pro-survival activity by the NRF2/HIPK2/p53 interplay (30-32). NRF2 regulates the transcription of drug metabolizing enzymes, antioxidant enzymes and drug transporters that allow cell adaptation and survival in oxidant stress conditions (33). When transiently activated in early tumorigenesis steps, NRF2 works as a cytoprotective factor and is associated with chemoprevention (34). By contrast, sustained NRF2 activation, as observed in NRF2-overexpressing cancers including lung cancer and CRC (35-37), is associated with an unfavorable prognosis (37,38), promotes metabolic activities that support cell proliferation and tumor growth, and serves a crucial role in determining drug resistance (34,39). Therefore, the NRF2 inhibitor brusatol, a natural quassinoid isolated from a traditional Chinese herbal medicine, *Brucea javanica*, and originally employed to treat amebiasis and malaria (40,41), has been proposed for cancer therapy in combination with current chemotherapies (42). In particular, it has been demonstrated that brusatol decreases the levels of NRF2 by ubiquitin-mediated degradation, impairs the cytoprotective response and sensitizes a broad spectrum of xenografts and cancer cells, such as lung adenocarcinoma A549 cells, cervix epithelioid carcinoma HeLa cells and triple-negative breast cancer MDA-MB-231 cells, to different chemotherapeutic drugs (43,44).

In the present study, tissue microarray (TMA) from patients with stage II CRC treated or not treated with adjuvant chemotherapy, and CRISPR/Cas9-mediated gene editing in CRC cells were used to address the contribution of HIPK2 in drug-response and its possible use as a predictive marker.

Materials and methods

Patients. The study group consisted of a retrospective series of stage II CRC cases (n=84) belonging to a cohort

of 270 patients with CRC who underwent curative-intent surgical resection at the IRCCS Regina Elena National Cancer Institute (Rome, Italy) between January 2000 and December 2013. The 84 patients with stage II CRC included in the present study had a median follow-up of 58.46 months (range, 8-144 months). The follow-up estimated using the Kaplan-Meier reverse method was 61 months (95% CI, 48-75 months), representing the 5-year period after which the patients that did not show disease relapse were no longer included in the follow-up. Tumors were staged according to the tumor-node-metastasis (TNM) system criteria (45), and all patients were diagnosed with stage II CRC (T3/T4, N0, M0). Clinical data were obtained from hospital medical records. As shown in Table I, 55 patients were males and 29 were females. The median age of the patients at the time of surgery was 67 years (range, 35-83 years), with 29 patients <65 and 55 patients >65 years old. Of the 84 patients, 24 were diagnosed with rectal cancer and 60 with colon cancer (23 patients had right-side colon cancer, 34 had left-side colon cancer and 3 had transverse colon cancer). Most of the patients were stage T3 (83%) and grade G2. According to the presence or absence of ≥ 1 high-risk features (T4 tumors, obstruction or perforation, <13 examined lymph nodes, positive margins, high-grade tumor, lympho-vascular and/or perineural invasion), 54 patients underwent surgery only and 30 underwent surgery plus adjuvant chemotherapy (Table II). The study was approved by the Central Ethics Committee of IRCCS Lazio (approval no. 1058/18). All patients signed an informed consent form for their tissues and clinical information to be used for research purposes based on previous approved study for tissue banking by the IFO Ethics Committee (July 7th 2003 and subsequent amendments and additions).

TMA construction. For this retrospective cross-sectional study, the CRC samples were histopathologically re-evaluated on hematoxylin/eosin stained slides and representative areas were marked prior to TMA construction. In cases where informative results on TMA were absent due to missing tissue, no tumor tissue or unsuccessful staining, the correspondent routine tissue section was re-analyzed. Two core cylinders (1-mm diameter) were taken from the CRC samples using a specific arraying device (Alphelys; Euroclone S.p.A.) and placed into two separate recipient paraffin blocks. In addition to tumor tissues, recipient blocks received normal colon tissues from the aforementioned patients (5 cm from tumor tissues) as negative controls. Sections (2- μ m-thick) of the resulting microarray blocks were made, transferred to SuperFrost Plus slides (Menzel-Gläser; VWR International, LLC) and used for immunohistochemistry (IHC).

IHC. IHC staining on TMA was manually performed using an anti-HIPK2 rat monoclonal antibody (moAb) 5C6 (46) [kindly provided by Professor M. Lienhard Schmitz (Justus-Liebig-University, Giessen, Germany)] diluted 1:50 and incubated at room temperature for 30 min, and detected using an anti-polyvalent diaminobenzidine staining system containing both blocking reagent and secondary antibody (ULTRATEK HRP; ScyTek Laboratories, Inc.) according to the manufacturer's protocol. Images were obtained at a magnification of x20 using a light microscope

Table I. Clinicopathological characteristics of patients with stage II colorectal cancer (n=84).

Characteristic	N	%
Age, years		
≤65	29	35
>65	55	65
Sex		
Male	55	65
Female	29	35
Tumor site		
Right colon	23	27
Left colon	34	40
Transverse colon	3	4
Rectum	24	29
T stage		
T3	71	84
T4	13	16
Grade		
G1	4	5
G2	69	82
G3	11	13
Adjuvant therapy		
No	54	64
Yes	30	36

T stage, tumor stage.

Table II. Type of adjuvant therapy administered to patients (n=30).

Type of adjuvant therapy	Number of treated patients
FOLFOX (folic acid + 5-FU + oxaliplatin)	9
FOLFOX + Vectibix	1
FOLFOX + Vectibix + radiotherapy	1
De Gramont (folic acid + 5-FU)	9
De Gramont + radiotherapy	1
Xeloda (capecitabine)	4
Xeloda + radiotherapy	2
Not specified ^a	3

^aDetails regarding the administered therapy were missing from the hospital record. 5-FU, 5-fluorouracil.

(DM2000 LED; Leica Microsystems GmbH) equipped with a software able to capture images (Leica Application Suite V4; version 4.8.0; Leica Microsystems GmbH). The percentages of HIPK2⁺ cells were evaluated by manually counting ≥200 cells per sample at high magnification (x40). Evaluation of the IHC results was performed independently by two blinded investigators.

Next generation sequencing (NGS). Paraffin-embedded tumor specimens, fixed for at least 24 h in 10% buffered formalin at room temperature, were reviewed for histological verification, as well as to ensure a minimum tumor cell content of 20%. Genomic DNA was extracted on the QIAcube[®] platform using the QIAamp DNA FFPE tissue kit (cat. no. 56404; Qiagen GmbH) according to the manufacturer's protocol. Library preparation was performed using an Ion Chef System (Thermo Fisher Scientific, Inc.) according to the manufacturer's instructions. Briefly, barcoded libraries were generated from 10 ng of DNA per sample using the Ion Ampliseq Library kit 2.0 and the Ion Ampliseq Cancer Hotspot Panel v2 (both from Thermo Fisher Scientific, Inc.). Amplified libraries were quantified using the Qubit 2.0 Fluorometer and the high sensitivity Qubit Assay kit (both from Thermo Fisher Scientific, Inc.) and combined to a final concentration of 100 pM. *TP53* sequencing was performed on an Ion S5 Sequencer using an Ion 530 Chip and an Ion 530 kit-Chef (all from Thermo Fisher Scientific, Inc.). In particular, to prepare DNA/RNA samples for sequencing, the following reagents and conditions were employed: Ion Ampliseq[™] Library kit plus (cat. no. A35907; Thermo Fisher Scientific, Inc.), Ion Ampliseq[™] Cancer hotspot panel v2 (cat. no. 4475346; Thermo Fisher Scientific, Inc.), Ion Xpress barcode Adapter 1-16 kit (cat. no. A4471250; Thermo Fisher Scientific, Inc.), AMPure XP 60 ml Agencourt (cat. no. A63881; Beckman Coulter, Inc.) and the Ion library TaqMan Quantification kit (cat. no. 4468802; Thermo Fisher Scientific, Inc.), which was also used to verify the quality/integrity of the processed samples. To prepare the sequencing library, the following reagents and kits were used (all from Thermo Fisher Scientific, Inc.): Ion S5[™] Chef Solutions (cat. no. A27754), Ion S5[™] Chef Supplies (cat. no. A27755), Ion 510[™] 520[™] 530[™] Chef Reagents (cat. no. A34018), Ion 530[™] Chip kit (cat. no. A27763), Ion S5[™] Sequencing solutions (cat. no. 27767), Ion S5[™] Sequencing reagents (cat. no. 27768). The loading concentration of the final library for DNA sequencing was 33 pM. The nucleotide length of sequencing was 200 bp and the direction of sequencing was paired end. Analysis was carried out using Ion Torrent Suite[™] Software v5.4 and Ion Reporter[™] v5.4 (both Thermo Fisher Scientific, Inc.). The Torrent Suite[™] Software was used to perform initial quality control, including chip loading density, median read length and number of mapped reads. The Coverage Analysis plugin was applied to all data and used to assess amplicon coverage for regions of interest. Variants were identified by Ion Reporter filter with a detection threshold of 5% variants. A cut-off of 200X coverage was applied to all analyses. Only single nucleotide variants resulting in a non-synonymous amino acid change or a premature stop codon, and all short indels resulting in either a frameshift or insertion/deletion of amino acids were selected. The NGS data have been uploaded at <https://gbox.garr.it/garrbox/index.php/s/GVmwVDVYy3FdtZn>.

Cells, reagents and transfection. Human HCT116 cells (kindly provided by Professor Bert Vogelstein (John Hopkins University School of Medicine, Baltimore, Maryland, USA), HeLa and HeLa HIPK2-null cells (47) (kindly provided by Professor M. Lienhard Schmitz) and RKO cells stably transfected with p-Super-control (Ctrl-i) or p-Super-HIPK2-short hairpin (sh)RNA (HIPK2-i) (21) [kindly provided by Professor

Gabriella D'Orazi (University of Chieti, Chieti, Italy)] were cultured in DMEM-GlutaMAX (HCT116 and HeLa cells) or RPMI-GlutaMAX (RKO cells) supplemented with 10% FBS, 100 U/ml penicillin and 100 $\mu\text{g}/\text{ml}$ streptomycin (all from Thermo Fisher Scientific, Inc.) and maintained in a humid incubator at 37°C in a 5% CO₂ environment. Stabilized patient-derived colorectal tumor-initiating cells, also known as cancer stem cells (CSCs), kindly provided by Professor Giorgio Stassi (University of Palermo, Palermo, Italy) and Professor Ruggero De Maria (Università Cattolica del Sacro Cuore, Rome, Italy), were cultured as previously described (48). Cells were X-irradiated with a dose of 20 Gy using an IBL437C irradiator (CIS Bio International) following the manufacturer's instructions. Cell death was measured using the Trypan blue exclusion assay (cat. no. 15250-061; Thermo Fisher Scientific, Inc.) following the manufacturer's protocol. The following drugs were used in the present study: 5-fluorouracil (5-FU) and oxaliplatin (OXA) (supplied by the Regina Elena Pharmacy), and brusatol (cat. no. SML1868; Sigma-Aldrich; Merck KGaA).

RNA interference was performed using a commercially available pool of three NRF2-specific small interfering (si)RNAs (cat. no. sc-37030) and a negative control siRNA (cat. no. sc-37007) (both from Santa Cruz Biotechnology, Inc.). HCT116 cells were transfected for 24 h at 37°C with 20 nM siRNA using RNAi-MAX Lipofectamine® (Invitrogen; Thermo Fisher Scientific, Inc.) according to the manufacturer's instructions. After 24 h of transfection, the cells were collected for subsequent analyses.

Cytotoxicity assay. Cell sensitivity to drugs was quantified using the Cell Proliferation kit II (Roche Diagnostics) according to the manufacturer's protocol. The method is based on the ability of viable cells to cleave the tetrazolium ring of 2,3-bis(2-methoxy-4-nitro-5-sulphophenyl)-2H-tetrazolium-5-carboxyanilide (XTT) inner salt yielding orange formazan crystals, which are soluble in aqueous solutions. Absorbance of formazan was measured at 450 nm and cell viability was expressed as a percentage of absorbance measured in the treated wells compared with that in the untreated control wells. HCT116 cells were treated at 37°C for 48 h with 2.5, 5, 12.5, 25, 50, 100 and 200 μM 5-FU and OXA. HeLa cells were treated at 37°C for 48 h with 5, 10, 25, 50 and 100 μM 5-FU and OXA. RKO cells were treated at 37°C for 48 h with 6.25, 12.5, 25, 50, 100, 200 and 400 μM 5-FU, and 6.25, 12.5, 25 and 50 μM OXA. Briefly, 8,000 cells/well (HCT116, HeLa and RKO) were seeded in 96-well plates and allowed to recover for 24 h before drug treatment. The drug concentrations and incubation times are also indicated in figures and legends. In combination experiments, brusatol (15 nM for Ctrl-Cas9 cells and 15 and 40 nM for HIPK2-Cas9 cells) was added 4 h before other chemotherapeutics. Subsequently, HCT116 Ctrl-Cas9 cells were treated with 1, 2.5, 5 and 10 μM 5-FU and OXA. HCT116 HIPK2-Cas9 cells were treated with 2.5, 5, 10, 20, 40 and 80 μM 5-FU, and 1, 2.5, 5, 10, 20 and 40 μM OXA. RKO-Ctrl and RKO-HIPK2i cells were treated with 3, 6, 12.5 and 25 μM 5-FU and OXA.

CRISPR-Cas9 genome editing and isolation of knock-out clonal cells. HCT116 cells were cultured in 6-well dishes to

reach 60-70% confluence and transfected using Lipofectamine® LTX reagent (Invitrogen; Thermo Fisher Scientific, Inc.) with plasmids pX459 pSpCas9(BB)-2A-Puro (cat. no. 62988; Addgene, Inc.) or pX459 Cas9-HIPK2 single guide (sg)RNA (5'-GTTCCAACCTGGGACATGACTG-3') (kindly provided by Professor M. Lienhard Schmitz), that targets the second exon of the HIPK2 gene affecting the kinase domain (47). Transfected cells were selected the next day using puromycin (ICN Biomedicals, Inc.) for 3 days. After selection, cells were cloned into a 96-well plate, expanded and screened for HIPK2 protein expression via western blotting using the aforementioned anti-HIPK2 rat 5C6 mAb. Genomic DNA was isolated from each clone using the Quick-gDNA MiniPrep kit (Zymo Research Corp.) according to the manufacturer's instructions. PCR was performed using the GoTaq DNA polymerase (Promega Corporation) using primers flanking the edited region of the *HIPK2* gene: HIPK2 exon 2 (294-753) forward, 5'-TGGCCTCACATGTGCAAGTT-3' and reverse, 5'-GCCCGCTTGCATTATTCTG-3'. The following thermocycling conditions were used: one cycle at 94°C for 3 min, followed by 40 cycles at 94°C for 3 min, 60°C for 30 sec and 72°C for 30 sec, and a final cycle at 72°C for 7 min. Sanger sequencing was performed on the genomic DNA PCR products by Eurofins Genomics.

Characterization of allele-specific mutations of HIPK2-Cas9 cells by TOPO TA cloning. To identify the allele-specific mutations of HIPK2 present in the HIPK2-Cas9 cells, the TOPO TA Cloning kit (Invitrogen; Thermo Fisher Scientific, Inc.) was used to directly insert Taq polymerase-amplified PCR products amplified from the edited region into the pcDNA 3.1/V5-His-TOPO vector according to the manufacturer's protocol. The TOPO cloning reactions were then transformed into TOP10 *E. coli* competent cells (Invitrogen; Thermo Fisher Scientific, Inc.). Single colonies were picked, and the plasmids were isolated by miniprep (Qiagen GmbH). Restriction analysis using *Bam*HI 10 U/ μl and *Xho*I 10 U/ μl (New England Biolabs, Inc.) was performed to determine the correct insertion of the PCR product. Correctly inserted clones were subsequently sequenced and analyzed for the presence of indel mutations. Nucleotide Blast alignment tool (49) was used to identify the indel mutations in the HIPK2-Cas9 cells. Bacterial agar plates were supplemented with 50 $\mu\text{g}/\text{ml}$ ampicillin (Sigma-Aldrich; Merck KGaA) and bacterial colonies were grown in LB broth (Invitrogen; Thermo Fisher Scientific, Inc.) with ampicillin (Sigma-Aldrich; Merck KGaA).

Reverse transcription-quantitative PCR. Total RNA was isolated using the RNeasy mini kit (cat. no. 74106; Qiagen GmbH) according to the manufacturer's protocol. RNA was reverse transcribed into cDNA using a M-MLTV RTase (cat. no. 28025-0.13; Invitrogen; Thermo Fisher Scientific, Inc.), 5X First Strand buffer (cat. no. Y02321; Invitrogen; Thermo Fisher Scientific, Inc.), 0.1 M DTT (cat. no. Y00147; Invitrogen; Thermo Fisher Scientific, Inc.), Primer random P(dN)₆ (cat. no. 1034731; Roche Diagnostics), RNase OUT 5,000 units (cat. no. 100000840; Invitrogen; Thermo Fisher Scientific, Inc.), 100 mM dCTP solution (cat. no. 55083), 100 mM dTTP solution (cat. no. 55085), 100 mM dATP solution (cat. no. 55082) and 100 mM dGTP solution (cat. no. 55084) (all

Invitrogen; Thermo Fisher Scientific, Inc.) for 90 min at 37°C. For quantitative PCR analysis, mRNA expression levels were evaluated using Power SYBR-Green PCR master mix (cat. no. 4367659; Applied Biosystems; Thermo Fisher Scientific, Inc.) with ABI Prism 7500HT Fast Real-Time PCR System Detector (Applied Biosystems; Thermo Fisher Scientific, Inc.). The thermocycling conditions were: one cycle at 50°C for 2 min; one cycle at 95°C for 10 min; 40 cycles at 95°C for 15 sec and 60°C for 1 min. Gene expression was quantified using the $2^{-\Delta\Delta C_q}$ method (50). GAPDH was used as the endogenous reference gene. Primer sequences were as follows: HIPK2 forward, 5'-AGGAAGAGTAAGCAGCACCAG-3' and reverse, 5'-TGCTGATGGTGTGACTGACTGA-3'; GAPDH forward, 5'-TCCCTGAGCTGAACGGGAAG-3' and reverse, 5'-GGAGGAGTGGGTGTCTGT-3'.

Western blotting. Whole-cell lysates were prepared using RIPA lysis buffer [50 mM Tris-HCl (pH 8), 150 mM NaCl, 0.5% sodium deoxycholate, 0.1% SDS, 1% NP-40 and 1 mM EDTA] supplemented with protease-inhibitor mix (Roche Diagnostics) and Halt Phosphatase Inhibitor Cocktail (cat. no. 1861277; Thermo Fisher Scientific, Inc.). The extracted proteins were quantified using the Bio-Rad Protein assay dye (cat. no. 5000006; Bio-Rad Laboratories, Inc.) and protein samples (20 μ g/lane) were separated via SDS-PAGE onto 4-12% gels (cat. no. NW04122B0X; Invitrogen; Thermo Fisher Scientific, Inc.) and then transferred onto nitrocellulose membranes (cat. no. 1620112; Bio-Rad Laboratories, Inc.). After blocking with 5% skimmed dry milk for 1 h at room temperature (cat. no. 170-6404; Bio-Rad Laboratories, Inc.), membranes were incubated overnight at 4°C with the aforementioned anti-HIPK2 rat moAb 5C6 (1:200), anti-NRF2 rabbit moAb (1:1,000; cat. no. ab62352; Abcam), anti-heat shock protein 70 (51) mouse moAb (1:1,000; cat. no. SAB4200714; Sigma-Aldrich; Merck KGaA), anti-GADPH mouse moAb (1:1,000; cat. no. sc-32233; Santa Cruz Biotechnology, Inc.), anti-poly (ADP-ribose) polymerase (PARP) rabbit polyclonal Ab (1:1,000; cat. no. 9542; Cell Signaling Technology, Inc.), anti-catalase mouse moAb (H-9; 1:500; cat. no. sc-271803; Santa Cruz Biotechnology, Inc.) and anti- α tubulin mouse moAb (1:1,000; cat. no. MAB-10285; Immunological Sciences). Following incubation with anti-mouse (cat. no. 7076), anti-rabbit (cat. no. 7074) (both Cell Signaling Technology, Inc.) or anti-rat IgG (cat. no. 31470; Thermo Fisher Scientific, Inc.) HRP-linked secondary antibodies (all 1:10,000) for 1 h at room temperature, immunoreactions were detected using an ECL WB Detection System (cat. no. RPN2209; GE Healthcare). Western blot bands were quantified using ImageJ v1.47 (National Institutes of Health).

Statistical analysis. SPSS version 21.0 (IBM Corp.) was used for statistical evaluations. Data are presented as the mean \pm standard error (SE). Cell viability data were statistically compared using the unpaired Student's t-test. The association between variables was tested using Pearson's χ^2 test or Fisher's exact test, as appropriate. The maximally selected Log-Rank statistics analysis was applied to the HIPK2 (using 5C6 Ab staining) continuous variable in order to estimate the

most appropriate cut-off values in which the amount of HIPK2 expression is able to divide patients into groups with different DFS probabilities (52). Survival curves were calculated using the Kaplan-Meier method and the log-rank test was used to assess differences between subgroups. $P \leq 0.05$ was considered to indicate a statistically significant difference.

Results

High HIPK2 expression is associated with an improved prognosis in adjuvant-treated patients with stage II CRC. To evaluate the contribution of HIPK2 in chemotherapy response in humans, HIPK2 expression was analyzed by IHC on cancer samples from patients with stage II CRC. After curative-intent surgical resection of the primary tumors, 30/84 patients were treated with adjuvant therapy according to the presence of ≥ 1 high-risk features (T4 tumors, obstruction or perforation, < 13 examined lymph nodes, positive margins, high-grade tumor, lympho-vascular and perineural invasion). The remaining 54 patients were only routinely checked for tumor recurrence. TMA sections of the 84 stage II CRC samples were labelled with anti-HIPK2 moAb and scored based on the number of HIPK2⁺ cells. Consistent with previous observations (53), TMAs from normal colon tissues exhibited a low level ($\leq 5\%$) of HIPK2⁺ cells (Fig. 1A). By contrast, TMAs from tumor samples exhibited a broad range of HIPK2 positivity with up to 50% positive cells (Fig. 1A). The cut-off value $> 10\%$ of HIPK2⁺ positive cells was statistically determined (52) and employed to divide the patients into two groups (HIPK2 ≤ 10 and > 10). In the total cohort of stage II CRC, 32% (27/84) of the cases exhibited HIPK2 > 10 , while analyzing the adjuvant-treated (Chemo) and untreated (No Chemo) subgroups separately, 47% (14/30) of the cases exhibited HIPK2 > 10 in the adjuvant-treated group and 24% (13/54) in the untreated one (Fig. 1B).

Next, the patients with HIPK2 ≤ 10 and > 10 were retrospectively evaluated for their 5-year disease-free survival (DFS) rate. When the total cohort of unselected stage II CRC cases was analyzed using Kaplan-Meier curves, a complete overlap was observed between the HIPK2 ≤ 10 and > 10 groups (Fig. 1C). Notably, when the patients were divided in the two subgroups of adjuvant-treated and untreated cases, the following was observed: In the adjuvant treated group, an improved prognosis was observed in the HIPK2 > 10 group compared with in the ≤ 10 group (Fig. 1D), while in the untreated group, an improved prognosis was observed with HIPK2 ≤ 10 compared with > 10 (Fig. 1E). Although a statistically significant difference was not reached due to the small number of patients in the subgroups, the divergent curves suggest an association between a high percentage of HIPK2⁺ cells and an improved response to therapy.

HIPK2-associated response to adjuvant therapy is independent of the TP53 gene status. A major target of HIPK2 in cell response to different types of stress is the tumor suppressor p53 (8-10). Mutations of the TP53 gene induce resistance to therapy in *in vitro* and *in vivo* models, as well as in patients with cancer (54,55). Thus, the present study investigated whether the aforementioned results may be associated with an enrichment in wild-type TP53 gene status in patients with a more favorable

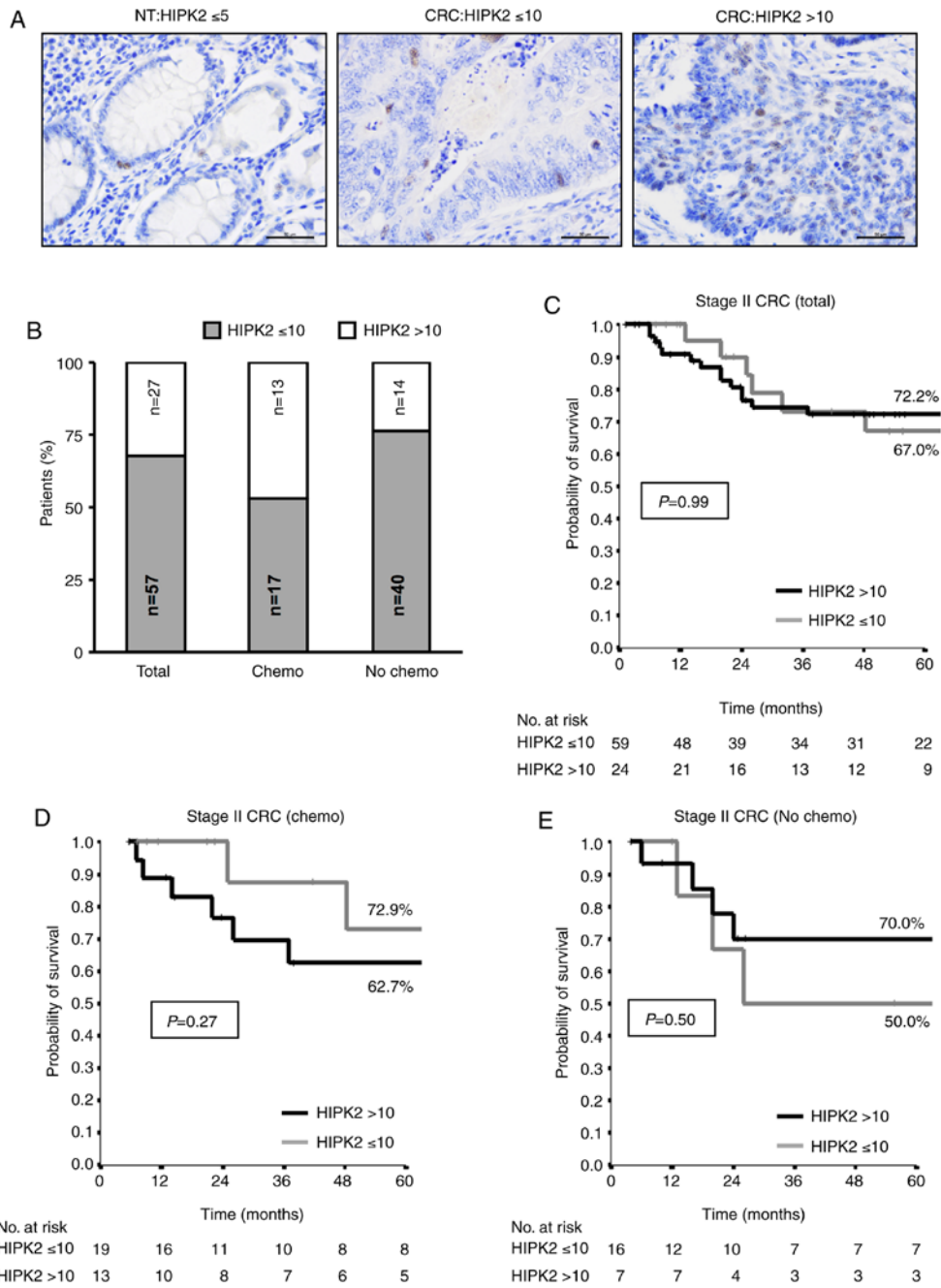


Figure 1. HIPK2 expression in patients with CRC. (A) Representative images of immunohistochemistry analyses with anti-HIPK2 moAb performed on NT colon tissue and CRC biopsies. Tumor samples are representative of HIPK2 ≤ 10 and > 10 expression. Scale bar, 50 μ m. (B) Total patients with stage II CRC (n=84) were stratified based on HIPK2 expression (≤ 10 and > 10). Next, patients were subdivided into adjuvant-treated (Chemo) and untreated (No Chemo) cases. The 'n' within the columns indicates the number of patients belonging to the respective group. (C) DFS evaluated by Kaplan-Meier curves on the panel of 84 patients with stage II CRC stratified based on HIPK2 expression. DFS evaluated by Kaplan-Meier curves stratified based on HIPK2 expression on the panel of (D) 30 treated patients (Chemo) and (E) 54 untreated patients (No Chemo) with adjuvant chemotherapy. NT, non-tumor; CRC, colorectal cancer; HIPK2, homeodomain-interacting protein kinase 2; DFS, disease-free survival.

prognosis. The *TP53* gene was sequenced by NGS in all 84 tumor samples. In the total cohort of stage II CRC, *TP53* mutations were detected in 38% (32/84) of cases (Fig. 2A). Similar percentages were maintained among adjuvant-treated and untreated patients, with mutations detected in 33.3% (10/30) and 40.7% (22/54) of cases, respectively (Fig. 2A). Next, the present study analyzed whether there was an association between HIPK2 expression and the *TP53* gene status. The percentage of cases with *TP53* mutations was 35% (20/57) in the HIPK2 ≤ 10 subgroup and 44% (12/27) in the HIPK2 > 10 group (Fig. 2B).

This trend was maintained when the adjuvant-treated and untreated groups were subdivided in the HIPK2 ≤ 10 and > 10 subgroups (Fig. 2C), indicating that the association between a high percentage of HIPK2⁺ cells and improved response to therapy may be independent of the *TP53* gene status.

Generation of HIPK2-null HCT116 CRC cells. To investigate the contribution of HIPK2 in chemotherapy response in CRC cells, the expression levels of endogenous HIPK2 were first evaluated in different CRC cells, including patient-derived

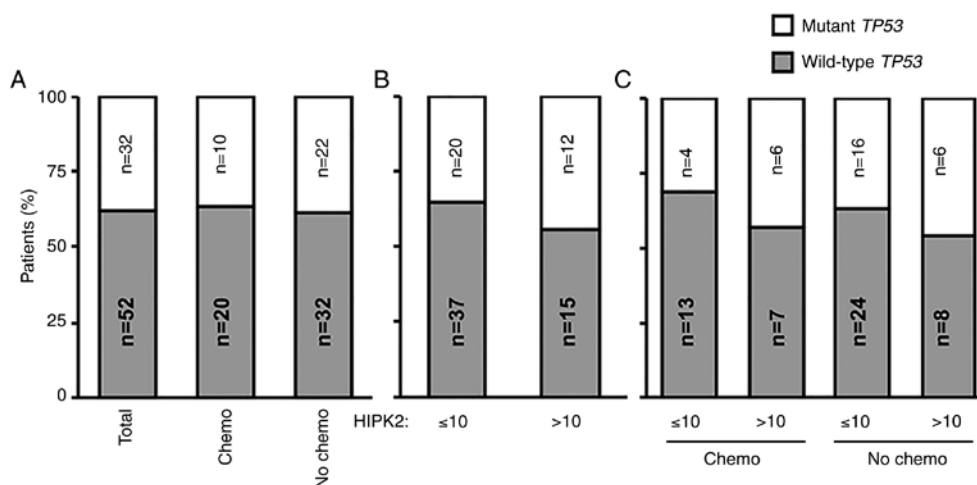


Figure 2. Next generation sequencing analysis of the *TP53* gene in patients with stage II CRC. The *TP53* gene was sequenced in the 84 patients with CRC, and its status (wild-type or mutant) is reported as a percentage in the different groups and subgroups. The 'n' within the columns indicates the number of patients belonging to the respective group. (A) Total patients (n=84) were subdivided into adjuvant-treated (Chemo) and untreated (No Chemo) groups. (B) Total patients (n=84) were subdivided based on HIPK2 expression, ≤ 10 and > 10 . (C) Patients were subdivided based on therapy and HIPK2 expression. CRC, colorectal cancer; HIPK2, homeodomain-interacting protein kinase 2.

CSCs, via western blotting. As shown in Fig. 3A, HIPK2 protein expression was detected in all cell lines and slightly increased after irradiation (used as a genotoxic stress to detect the activation of HIPK2) (14) in three out of seven cell lines (HCT116, CSC1 and RKO). Next, the CRISPR/Cas9 technology was used to generate HIPK2-null HCT116 CRC cells. HCT116 cells were transfected with the Cas9-control plasmid (HCT116^{Ctrl-Cas9}) or the Cas9-HIPK2 sgRNA plasmid carrying a sgRNA targeting the second exon of the *HIPK2* gene (HCT116^{HIPK2-Cas9}) (Fig. 3B). After puromycin selection, single-cell clones were expanded and screened for HIPK2 protein expression via western blotting. Compared with the HCT116^{Ctrl-Cas9} cells, the HIPK2 specific band of 130 kDa was not detectable in the HCT116^{HIPK2-Cas9} cells (Fig. 3C). As a further control, the genomic DNA from each clone was isolated and amplified using PCR with primers flanking the edited region in the *HIPK2* gene, within exon 2. The PCR products were verified by Sanger sequencing to determine the precise editing that occurred in each clone. From the sequencing analysis, it was confirmed that a frameshift mutation within exon 2, leading to a premature stop codon, was present in both HIPK2 alleles of HCT116^{HIPK2-Cas9} cells (Fig. S1).

HIPK2-knockout induces resistance of CRC cells to 5-FU and OXA. 5-FU and OXA are frequently used in the treatment of CRC, including stage II cases (56). To investigate the contribution of HIPK2 in the sensitivity of CRC cells to these drugs, HCT116^{Ctrl-Cas9} and HCT116^{HIPK2-Cas9} cells (herein Ctrl-Cas9 and HIPK2-Cas9 cells) were treated with increasing concentrations of 5-FU or OXA and cell viability was assessed using XTT 48 h post-treatment. The results revealed that, compared with Ctrl-Cas9 cells, HIPK2-knockout significantly decreased cell sensitivity to both drugs (Fig. 4A). Similar results were obtained with Ctrl-Cas9 and HIPK2-Cas9 HeLa cells (Fig. S2A) and CRC RKO cells stably transfected with an HIPK2-specific shRNA (21) (Fig. S2B), indicating that the drug resistance induced by HIPK2 depletion is not cell-specific and independent of the gene-depletion method.

Next, the number of dead cells after 48 h of treatment was evaluated. As expected, a dose-dependent increment in cell death was observed in the Ctrl-Cas9 cells; by contrast, no increase in cell death was observed in the HIPK2-Cas9 cells (Fig. 4B). These results were confirmed by PARP cleavage analysis. As shown in Fig. 4C, PARP cleavage was clearly detectable in Ctrl-Cas9 cells in the presence of either drug, whereas it was scarcely detectable in HIPK2-Cas9 cells, even though they had been treated with higher doses of OXA and 5-FU than control cells due to their drug-resistance. Consistently with previous data (10), the present results revealed that HIPK2-knockout induced resistance to 5-FU and OXA in HCT116 CRC cells.

Chemoresistance induced by HIPK2-knockout is not overcome using the NRF2 inhibitor brusatol. Sustained activation of NRF2 contributes to chemoresistance in different types of human cancer, including CRC (57,58), and NRF2 inactivation by brusatol sensitizes several cancer cells to different chemotherapeutic drugs, such as CRC cells to Adriamycin or lung cancer cells to cisplatin (30,43,44). Therefore, brusatol was used in combination with 5-FU and OXA to assess the effect in the current cellular system. It was revealed that brusatol decreased the protein expression levels of NRF2 in HCT116 cells in a dose-dependent manner (Fig. 5A). Subsequently, the effect of brusatol alone was analyzed to identify a dose that did not affect cell survival on its own. Ctrl-Cas9 and HIPK2-Cas9 HCT116 cells were treated with increasing concentrations of brusatol (15-100 nM), and cell viability was assessed using XTT. The results revealed that viability in Ctrl-Cas9 cells was significantly decreased in response to doses of brusatol > 20 nM, while HIPK2-Cas9 cells were insensitive to brusatol even at the highest tested concentration (100 nM; Fig. 5B). Thus, a brusatol dose of 15 nM that did not affect cell viability in Ctrl-Cas9 cells was employed for combination experiments. Due to the observed brusatol resistance, HIPK2-Cas9 cells were also treated with a higher dose (40 nM). After 4 h of brusatol treatment, Ctrl-Cas9 and

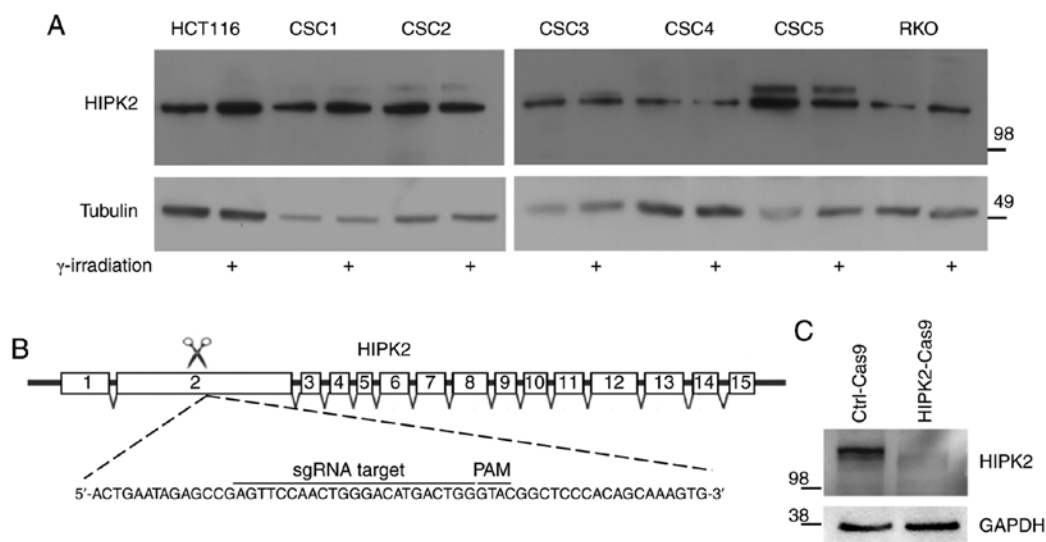


Figure 3. HIPK2 expression in CRC cells and its genome editing using CRISPR/Cas9 technology. (A) Endogenous HIPK2 expression levels before and after irradiation with 20 Gy to induce genotoxic damage in a panel of CRC cells, including patient-derived CSCs detected by WB. Tubulin was used as the loading control. (B) Schematic structure of the human *HIPK2* gene with introns and exons. The sgRNA-targeted site in exon 2 is reported. (C) WB analysis for HIPK2 expression was performed in Ctrl-Cas9 and HIPK2-Cas9 HCT116 cells. The 130 kDa band of HIPK2 is detectable only in the control cells. GAPDH was used as a loading control. CRC, colorectal cancer; HIPK2, homeodomain-interacting protein kinase 2; CSC, cancer stem cell; Ctrl, control; WB, western blotting; sgRNA, single guide RNA.

HIPK2-Cas9 cells were treated with increasing concentrations of 5-FU and OXA and analyzed using XTT. It was observed that brusatol significantly increased cell sensitivity to both drugs in HIPK2-proficient cells (Fig. 5C). However, no significant effect was induced by brusatol treatment, even at the 40 nM dose, in HIPK2-Cas9 cells (Fig. 5D), indicating that brusatol did not overcome the resistance to 5-FU and OXA in HIPK2-knockout cells. Similar results were obtained using the Ctrl-i and HIPK2-i RKO cells (Fig. S3), excluding the possibility of cell-specificity and depletion strategy-specificity. Next, to explore the potential mechanism of this divergent response to brusatol, the present study analyzed whether the recently described transcriptional regulation of HIPK2 by NRF2 (26) was also detectable in HCT116 cells. It was found that NRF2 depletion by RNA interference resulted in repression of HIPK2 expression both at the protein (Fig. 5E) and mRNA (Fig. 5F) levels, confirming the NRF2-mediated transcriptional regulation of HIPK2. Additionally, a constitutive decrease in the expression levels of NRF2 and its transcriptional target, catalase, was observed in HIPK2-Cas9 cells (Fig. 5G). This highlighted a crosstalk between NRF2 and HIPK2, suggesting that brusatol may be ineffective in HIPK2-Cas9 cells due to the already decreased expression levels of NRF2. Overall, the present data suggested that HIPK2 may be required for the chemotherapy sensitization induced by brusatol.

Discussion

Stage II CRC is an early-stage CRC with a low risk of recurrence. While therapeutic strategies for the more advanced CRC stages III and IV are standardized, those for stage II remain questionable (5). Intense efforts have focused on developing molecular biomarkers useful as prognostic factors for identifying stage II patients at increased risk of disease recurrence,

but not for predicting whether stage II patients would truly benefit from adjuvant chemotherapy (3).

Since HIPK2 is a key player in the cellular response to different DNA damage-inducing stimuli, including genotoxic drugs, it is consequently involved in the response of tumor cells to chemotherapy (10,59). The present study analyzed the role of HIPK2 in response to chemotherapy and assessed its predictive role on DFS of patients with stage II CRC. Despite limitations due to the small sample size that did not allow to obtain statistically significant differences, the 5-year DFS curves displayed two opposite trends in adjuvant-treated and untreated subgroups. In the untreated subgroup, a high percentage of HIPK2⁺ cells in the tumor samples (HIPK2 >10) was associated with a lower DFS time than in those with HIPK2 ≤10. By contrast, HIPK2 >10 cases in the adjuvant-treated subgroup exhibited a higher DFS time than the HIPK2 ≤10 cases. The current data are consistent with the pro-apoptotic and chemosensitivity functions of HIPK2 reported in several types of cancer cells *in vitro* and in xenografts, such as esophageal squamous cell carcinoma cells (19). These data suggest that HIPK2 may work in a similar manner in experimental systems and at least in early stage CRC. Furthermore, the present study generated HIPK2-null HCT116 CRC cells using the CRISPR/Cas9 technology and assessed their sensitivity to 5-FU and OXA.

Conflicting roles of HIPK2 have been described in relation to cancer, implicating a tumor-specific and context-dependent activity of HIPK2, as well as suggesting that it may work as a versatile protein, which in turn acts as a fine-tuner of different signaling pathways (60). For instance, a redox-regulated HIPK2 acetylation may restrict its pro-apoptotic activity (28). HIPK2 may regulate the same target differently, including the oncosuppressor p53, depending on the cellular context and type, as well as on the stimulus intensity (28). In addition, mutations in the *TP53* gene contribute to both cancer

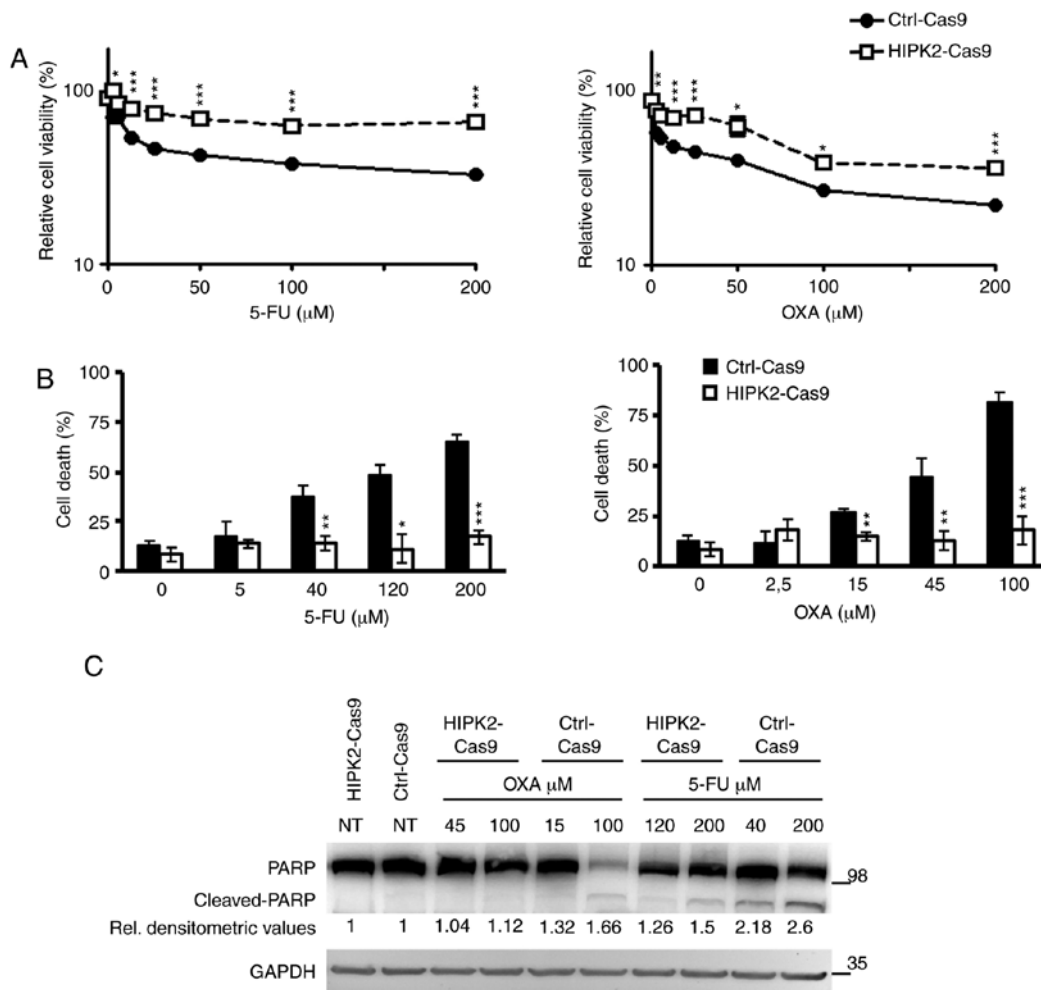


Figure 4. HIPK2 expression and drug response. (A) Ctrl-Cas9 and HIPK2-Cas9 HCT116 cells (8×10^3 /well) were exposed to increasing doses of 5-FU (left panel) and OXA (right panel) for 48 h, and cell viability was measured by XTT assay. For each point, the percentage compared with the untreated sample was calculated. Each point represents the mean \pm SE of cell viability at each dose of 5-FU and OXA. (B) Ctrl-Cas9 and HIPK2-Cas9 HCT116 cells were treated with increasing doses of 5-FU (left panel) and OXA (right panel) for 48 h, and counted by Trypan blue-exclusion test. The percentage of cell death for each sample is reported as the mean \pm SE of three independent experiments. * $P < 0.05$; ** $P < 0.01$; *** $P < 0.001$. (C) PARP cleavage was detected by western blotting in Ctrl-Cas9 and HIPK2-Cas9 HCT116 cells treated with the indicated doses of 5-FU and OXA for 48 h from one representative experiment. GAPDH was used as a loading control. Densitometric values reported below the PARP blot were first normalized according to protein amount in the loading control, then calculated taking the relative NT control as the reference value. ImageJ software was employed. SE, standard error; PARP, poly (ADP-ribose) polymerase; 5-FU, 5-fluorouracil; OXA, oxaliplatin; HIPK2, homeodomain-interacting protein kinase 2; Ctrl, control; NT, non-tumor; XTT, 2,3-bis-(2-methoxy-4-nitro-5-sulfophenyl)-2H-tetrazolium-5-carboxanilide.

development (61) and resistance to cancer therapy (62). Thus, the present study investigated whether the *TP53* gene status could explain the different outcomes between adjuvant-treated and untreated subgroups. No enrichment of the wild-type *TP53* gene was observed in the best chemo-responding subgroup. By contrast, a mild, although not statistically significant, accumulation of *TP53* mutations was observed in adjuvant-treated patients with HIPK2 >10 and a more favorable prognosis, suggesting that the drug sensitivity in cells expressing high HIPK2 expression may be independent of the *TP53* gene status.

Since the *TP53* status did not explain the difference in drug sensitivity, Ctrl-Cas9 and HIPK2-Cas9 HCT116 cells were used to evaluate the possible contribution of the cytoprotective factor NRF2. This hypothesis stems from different considerations, including the constitutive activation of NRF2 in CRC, the role of NRF2 in tumor progression and drug resistance (58), and the recently identified pro-survival crosstalk

between NRF2 and HIPK2 (29). NRF2 is considered a potential therapeutic target for improving chemotherapy sensitivity of cancer cells (63), and the NRF2 inhibitor brusatol has been demonstrated to possess biological activity in various types of cancer, including CRC (64), and to improve their chemotherapeutic response (30). The previously reported brusatol-mediated repression of NRF2 expression (43) and the NRF2-mediated transcriptional regulation of HIPK2 (29) were confirmed in the present study. Notably, when brusatol was used in combination with 5-FU and OXA, increased chemosensitivity was only observed in the HIPK2-proficient cells, while no effect was detected in the HIPK2-null cells, which exhibited decreased NRF2 expression, in accordance with the previous results of the crosstalk between HIPK2 and NRF2 (26,29). The current results are in line with the hypothesis that targeting NRF2 may restore HIPK2 apoptotic activity by increasing the generation of reactive oxygen species (32), which strongly indicates that NRF2 and HIPK2

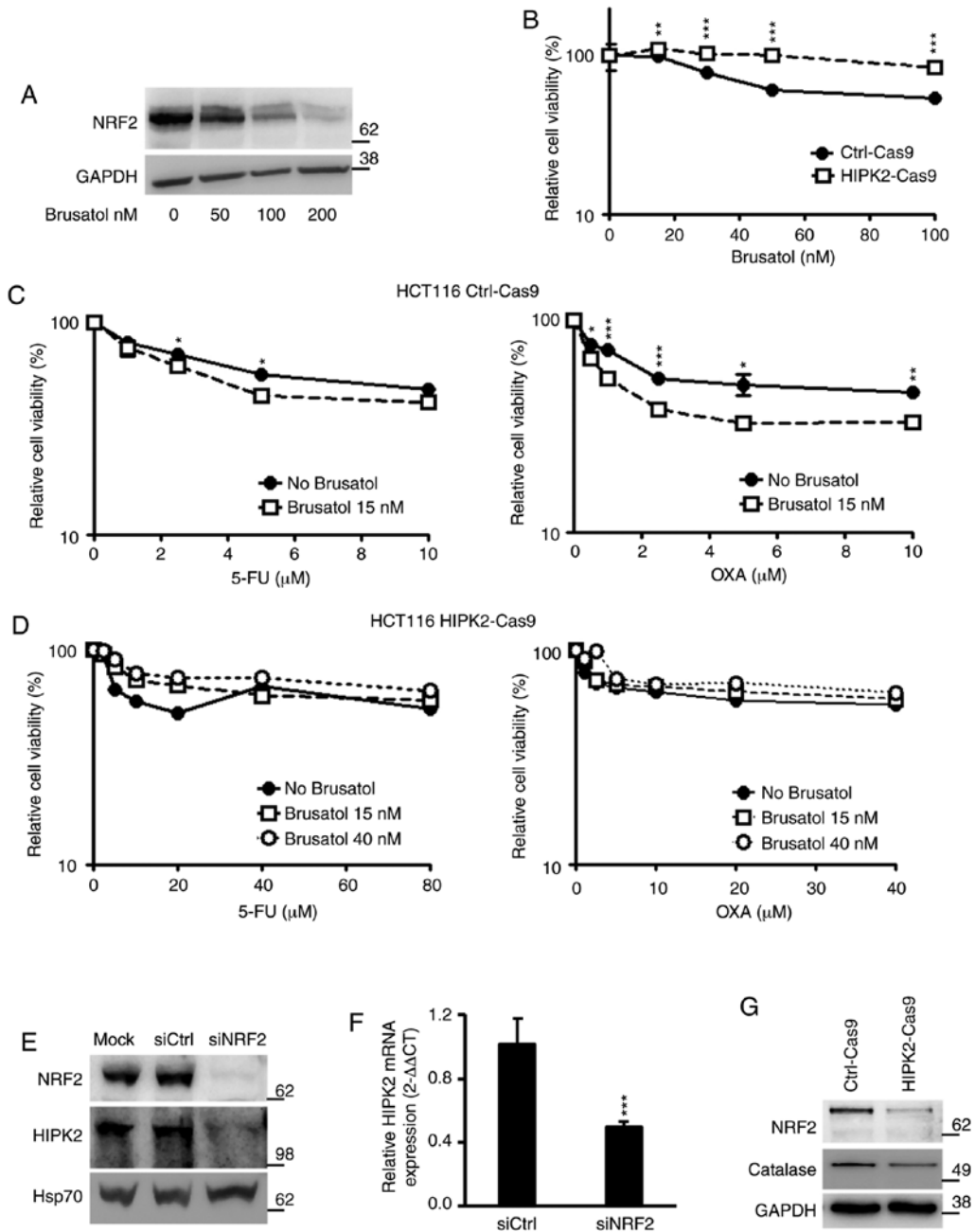


Figure 5. HIPK2 expression and drug response in combination with NRF2 inhibition. (A) Parental, HIPK2-proficient HCT116 cells were treated with increasing doses of brusatol for 4 h, and NRF2 expression was analyzed by WB. GAPDH was used as the protein loading control. (B) Ctrl-Cas9 and HIPK2-Cas9 HCT116 cells were treated with increasing doses of brusatol, and cell viability was assessed by XTT after 48 h. Each point represents the percentage (mean \pm SE) of cell viability compared with the untreated sample. (C) Ctrl-Cas9 cells were treated with increasing doses of 5-FU (left panel) and OXA (right panel) for 48 h in the presence or absence of brusatol (15 nM) added 4 h before the other drugs. The percentage of cell viability compared with the untreated sample (mean \pm SE) was assessed by XTT. (D) HIPK2-Cas9 cells were treated with 5-FU (left panel) and OXA (right panel) for 48 h in the presence or absence of brusatol. Two doses of brusatol (15 and 40 nM) were employed on these cells due to their resistance. (E) siNRF2 and siCtrl were transfected to interfere with NRF2 expression in parental, HIPK2-proficient HCT116 cells. NRF2 and HIPK2 expression levels were assessed by WB. HSP70 was used as the protein loading control. (F) HCT116 cells transfected with siNRF2 or siCtrl RNAs were analyzed by reverse transcription-quantitative PCR to quantify HIPK2 mRNA expression. (G) Protein expression levels of NRF2 and catalase were detected by WB in Ctrl-Cas9 and HIPK2-Cas9 HCT116 cells. GAPDH was used as the protein loading control. * P <0.05; ** P <0.01; *** P <0.001. XTT, 2,3-bis-(2-methoxy-4-nitro-5-sulphophenyl)-2H-tetrazolium-5-carboxanilide; WB, western blotting; si, small interfering; Ctrl, control; SE, standard error; 5-FU, 5-fluorouracil; OXA, oxaliplatin; HIPK2, homeodomain-interacting protein kinase 2; NRF2, nuclear factor erythroid 2-related factor 2; HSP70, heat shock protein 70.

expression may be considered as useful markers for selecting therapeutic options.

In conclusion, the present data revealed that HIPK2 expression was associated with chemo-response in early-stage CRC, which represents an initial step toward defining a novel predictive marker for patients with stage II

CRC who may benefit from adjuvant therapy. In addition, the current data demonstrated that the inhibition of NRF2 induced an increase in chemotherapy response only when HIPK2 was expressed, indicating that HIPK2 may be a crucial factor to be considered for combination therapy with NRF2 modulators.

Acknowledgements

The authors would like to thank Professor M. Lienhard Schmitz (Justus-Liebig-University, Giessen, Germany), Professor Bert Vogelstein (John Hopkins University School of Medicine, Baltimore, Maryland, USA), Professor Gabriella D'Orazi (University of Chieti, Chieti, Italy), Professor Giorgio Stassi (University of Palermo, Palermo, Italy) and Professor Ruggero De Maria (Università Cattolica del Sacro Cuore, Rome, Italy) for kindly gifting their cell lines and reagents. Additionally, the authors would like to thank Dr Maria Pia Gentileschi and Dr Ilaria Viridia from the IRCCS Regina Elena National Cancer Institute for their technical assistance, and Mrs. Tania Merlino from the Scientific Direction of the IRCCS Regina Elena National Cancer Institute for language editing.

Funding

The present study was supported by grants from Ministero della Salute (grant no. PE-2016-02361181) and Ricerca Corrente IRE.

Availability of data and materials

The datasets used and/or analyzed during the current study are available from the corresponding author on reasonable request

Authors' contributions

SS, AV and GDR designed the study. AV and MDS performed the experiments. CAA performed TMA and NGS. SB performed NGS. GDR designed and supervised the genome editing experiments. MDS generated the CRISPR/Cas9-modified cells. IS, SB and MM analyzed the clinical and NGS data. AV prepared the figures. AV and SS wrote the manuscript. GDR revised the manuscript. SS and GDR jointly supervised this work as co-last authors. All authors have read and approved the final version of the manuscript.

Ethics approval and consent to participate

Specimen collection was approved by the Central Ethics Committee of IRCCS Lazio (approval no. 1058/18). All patients signed an informed consent form for their tissues and clinical information to be used for research purposes based on previous approved study for tissue banking by the IFO Ethics Committee (July 7th 2003 and subsequent amendments and additions).

Patient consent for publication

Not applicable.

Competing interests

The authors declare that they have no competing interests.

References

- Siegel RL, Miller KD, Goding Sauer A, Fedewa SA, Butterly LF, Anderson JC, Cercek A, Smith RA and Jemal A: Colorectal cancer statistics, 2020. *CA Cancer J Clin* 70: 145-164, 2020.
- Gunderson LL, Jessup JM, Sargent DJ, Greene FL and Stewart AK: Revised TN categorization for colon cancer based on national survival outcomes data. *J Clin Oncol* 28: 264-271, 2010.
- Lee JJ and Chu E: Adjuvant chemotherapy for stage II colon cancer: The debate goes on. *J Oncol Pract* 13: 245-246, 2017.
- Knapen DG, Cherny NI, Zygoura P, Latino NJ, Douillard JY, Dafni U, de Vries EGE and de Groot DJ: Lessons learnt from scoring adjuvant colon cancer trials and meta-analyses using the ESMO-magnitude of clinical benefit scale V.1.1. *ESMO Open* 5: e000681, 2020.
- Varghese A: Chemotherapy for stage II colon cancer. *Clin Colon Rectal Surg* 28: 256-261, 2015.
- Guinney J, Dienstmann R, Wang X, de Reyniès A, Schlicker A, Soneson C, Marisa L, Roepman P, Nyamundanda G, Angelino P, *et al*: The consensus molecular subtypes of colorectal cancer. *Nat Med* 21: 1350-1356, 2015.
- Wolff RK, Hoffman MD, Wolff EC, Herrick JS, Sakoda LC, Samowitz WS and Slattery ML: Mutation analysis of adenomas and carcinomas of the colon: Early and late drivers. *Genes Chromosomes Cancer* 57: 366-376, 2018.
- D'Orazi G, Cecchinelli B, Bruno T, Manni I, Higashimoto Y, Saito S, Gostissa M, Coen S, Marchetti A, Del Sal G, *et al*: Homeodomain-interacting protein kinase-2 phosphorylates p53 at Ser 46 and mediates apoptosis. *Nat Cell Biol* 4: 11-19, 2002.
- Hofmann TG, Möller A, Sirma H, Zentgraf H, Taya Y, Dröge W, Will H and Schmitz ML: Regulation of p53 activity by its interaction with homeodomain-interacting protein kinase-2. *Nat Cell Biol* 4: 1-10, 2002.
- Puca R, Nardinocchi L, Givol D and D'Orazi G: Regulation of p53 activity by HIPK2: Molecular mechanisms and therapeutical implications in human cancer cells. *Oncogene* 29: 4378-4387, 2010.
- Blaquiere JA and Verheyen EM: Homeodomain-interacting protein kinases: Diverse and complex roles in development and disease. *Curr Top Dev Biol* 123: 73-103, 2017.
- Nardinocchi L, Puca R, Givol D and D'Orazi G: HIPK2-a therapeutical target to be (re)activated for tumor suppression: Role in p53 activation and HIF-1 α inhibition. *Cell Cycle* 9: 1270-1275, 2010.
- D'Orazi G, Rinaldo C and Soddu S: Updates on HIPK2: A resourceful oncosuppressor for clearing cancer. *J Exp Clin Cancer Res* 31: 63, 2012.
- Hofmann TG, Glas C and Bitomsky N: HIPK2: A tumour suppressor that controls DNA damage-induced cell fate and cytokinesis. *Bioessays* 35: 55-64, 2013.
- Kuwano Y, Nishida K, Akaike Y, Kurokawa K, Nishikawa T, Masuda K and Rokutan K: Homeodomain-interacting protein kinase-2: A critical regulator of the DNA damage response and the epigenome. *Int J Mol Sci* 17: 1638, 2016.
- Lavra L, Rinaldo C, Ulivieri A, Luciani E, Fidanza P, Giacomelli L, Bellotti C, Ricci A, Trovato M, Soddu S, *et al*: The loss of the p53 activator HIPK2 is responsible for galectin-3 overexpression in well differentiated thyroid carcinomas. *PLoS One* 6: e20665, 2011.
- Nodale C, Sheffer M, Jacob-Hirsch J, Folgiero V, Falcioni R, Aiello A, Garufi A, Rechavi G, Givol D and D'Orazi G: HIPK2 downregulates vimentin and inhibits breast cancer cell invasion. *Cancer Biol Ther* 13: 198-205, 2012.
- Tan M, Gong H, Zeng Y, Tao L, Wang J, Jiang J, Xu D, Bao E, Qiu J and Liu Z: Downregulation of homeodomain-interacting protein kinase-2 contributes to bladder cancer metastasis by regulating Wnt signaling. *J Cell Biochem* 115: 1762-1767, 2014.
- Zhang Z, Wen P, Li F, Yao C, Wang T, Liang B, Yang Q, Ma L and He L: HIPK2 inhibits cell metastasis and improves chemosensitivity in esophageal squamous cell carcinoma. *Exp Ther Med* 15: 1113-1118, 2018.
- Chen P, Duan X, Li X, Li J, Ba Q and Wang H: HIPK2 suppresses tumor growth and progression of hepatocellular carcinoma through promoting the degradation of HIF-1 α . *Oncogene* 39: 2863-2876, 2020.
- D'Orazi G, Sciulli MG, Di Stefano V, Riccioni S, Frattini M, Falcioni R, Bertario L, Sacchi A and Patrignani P: Homeodomain-interacting protein kinase-2 restrains cytosolic phospholipase A2-dependent prostaglandin E2 generation in human colorectal cancer cells. *Clin Cancer Res* 12: 735-741, 2006.
- Nardinocchi L, Puca R, Sacchi A and D'Orazi G: Inhibition of HIF-1 α activity by homeodomain-interacting protein kinase-2 correlates with sensitization of chemoresistant cells to undergo apoptosis. *Mol Cancer* 8: 1, 2009.

23. Lin J, Zhang Q, Lu Y, Xue W, Xu Y, Zhu Y and Hu X: Downregulation of HIPK2 increases resistance of bladder cancer cell to cisplatin by regulating Wip1. *PLoS One* 9: e98418, 2014.
24. Al-Beiti MA and Lu X: Expression of HIPK2 in cervical cancer: Correlation with clinicopathology and prognosis. *Aust N Z J Obstet Gynaecol* 48: 329-336, 2008.
25. Deshmukh H, Yeh TH, Yu J, Sharma MK, Perry A, Leonard JR, Watson MA, Gutmann DH and Nagarajan R: High-resolution, dual-platform aCGH analysis reveals frequent HIPK2 amplification and increased expression in pilocytic astrocytomas. *Oncogene* 27: 4745-4751, 2008.
26. Cheng Y, Al-Beiti MA, Wang J, Wei G, Li J, Liang S and Lu X: Correlation between homeodomain-interacting protein kinase 2 and apoptosis in cervical cancer. *Mol Med Rep* 5: 1251-1255, 2012.
27. Imberg-Kazdan K, Ha S, Greenfield A, Poultney CS, Bonneau R, Logan SK and Garabedian MJ: A genome-wide RNA interference screen identifies new regulators of androgen receptor function in prostate cancer cells. *Genome Res* 23: 581-591, 2013.
28. de la Vega L, Grishina I, Moreno R, Krüger M, Braun T and Schmitz ML: A redox-regulated SUMO/acetylation switch of HIPK2 controls the survival threshold to oxidative stress. *Mol Cell* 46: 472-483, 2012.
29. Torrente L, Sanchez C, Moreno R, Chowdhry S, Cabello P, Isono K, Koseki H, Honda T, Hayes JD, Dinkova-Kostova AT and de la Vega L: Crosstalk between NRF2 and HIPK2 shapes cytoprotective responses. *Oncogene* 36: 6204-6212, 2017.
30. Garufi A, Traversi G, Gilardini Montani MS, D'Orazi V, Pistrutto G, Cirone M and D'Orazi G: Reduced chemotherapeutic sensitivity in high glucose condition: Implication of antioxidant response. *Oncotarget* 10: 4691-1702, 2019.
31. Garufi A, Baldari S, Pettinari R, Gilardini Montani MS, D'Orazi V, Pistrutto G, Crispini A, Giorno E, Toietta G, Marchetti F, *et al*: A ruthenium(II)-curcumin compound modulates NRF2 expression balancing the cancer cell death/survival outcome according to p53 status. *J Exp Clin Cancer Res* 39: 122, 2020.
32. D'Orazi G, Garufi A and Cirone M: Nuclear factor erythroid 2 (NF-E2) p45-related factor 2 interferes with homeodomain-interacting protein kinase 2/p53 activity to impair solid tumors chemosensitivity. *IUBMB Life* 72: 1634-1639, 2020.
33. Vomund S, Schäfer A, Parnham MJ, Brüne B and von Knethen A: Nrf2, the master regulator of anti-oxidative responses. *Int J Mol Sci* 18: 2772, 2017.
34. Wu S, Lu H and Bai Y: Nrf2 in cancers: A double-edged sword. *Cancer Med* 8: 2252-2267, 2019.
35. Li CQ, Kim MY, Godoy LC, Thiantanawat A, Trudel LJ and Wogan GN: Nitric oxide activation of Keap1/Nrf2 signaling in human colon carcinoma cells. *Proc Natl Acad Sci USA* 106: 14547-14551, 2009.
36. Hu T, Yao Y, Yu S, Guo H, Han L, Wang W, Tian T, Hao Y, Liu Z, Nan K and Wang S: Clinicopathologic significance of CXCR4 and Nrf2 in colorectal cancer. *J Biomed Res* 27: 283-290, 2013.
37. Lee YJ, Kim WI, Bae JH, Cho MK, Lee SH, Nam HS, Choi IH and Cho SW: Overexpression of Nrf2 promotes colon cancer progression via ERK and AKT signaling pathways. *Ann Surg Treat Res* 98: 159-167, 2020.
38. Yang Q, Deng H, Xia H, Xu M, Pan G, Mao J, Tao S, Yamanaka K and An Y: High NF-E2-related factor 2 expression predicts poor prognosis in patients with lung cancer: A meta-analysis of cohort studies. *Free Radic Res*: Jul 24, 2019 (Epub ahead of print). doi: 10.1080/10715762.2019.1642472.
39. Wang YY, Chen J, Liu XM, Zhao R and Zhe H: Nrf2-mediated metabolic reprogramming in cancer. *Oxid Med Cell Longev* 2018: 9304091, 2018.
40. Bawm S, Matsuura H, Elkhateeb A, Nabeta K, Subeki, Nonaka N, Oku Y and Katakura K: In vitro antitrypanosomal activities of quassinoid compounds from the fruits of a medicinal plant, *Brucea javanica*. *Vet Parasitol* 158: 288-294, 2008.
41. Zhao M, Lau ST, Leung PS, Che CT and Lin ZX: Seven quassinoids from fructus bruceae with cytotoxic effects on pancreatic adenocarcinoma cell lines. *Phytother Res* 25: 1796-1800, 2011.
42. Panieri E, Buha A, Telkoparan-Akillilar P, Cevik D, Kouretas D, Veskokis A, Skaperda Z, Tsatsakis A, Wallace D, Suzen S and Saso L: Potential applications of NRF2 modulators in cancer therapy. *Antioxidants (Basel)* 9: 193, 2020.
43. Ren D, Villeneuve NF, Jiang T, Wu T, Lau A, Toppin HA and Zhang DD: Brusatol enhances the efficacy of chemotherapy by inhibiting the Nrf2-mediated defense mechanism. *Proc Natl Acad Sci USA* 108: 1433-1438, 2011.
44. Cai SJ, Liu Y, Han S and Yang C: Brusatol, an NRF2 inhibitor for future cancer therapeutic. *Cell Biosci* 9: 45, 2019.
45. Amin MB, Edge S, Greene F, Byrd DR, Brookland RK, Washington MK, Gershenwald JE, Compton CC, Hess KR, Sullivan DC, *et al* (eds): *AJCC Cancer Staging Manual*. Springer, New York, NY, pp252-254, 2017.
46. de la Vega L, Hornung J, Kremmer E, Milanovic M and Schmitz ML: Homeodomain-interacting protein kinase 2-dependent repression of myogenic differentiation is relieved by its caspase-mediated cleavage. *Nucleic Acids Res* 41: 5731-5745, 2013.
47. Ritter O and Schmitz ML: Differential intracellular localization and dynamic nucleocytoplasmic shuttling of homeodomain-interacting protein kinase family members. *Biochim Biophys Acta Mol Cell Res* 1866: 1676-1686, 2019.
48. Manic G, Signore M, Sistigu A, Russo G, Corradi F, Siteni S, Musella M, Vitale S, De Angelis ML, Amoreo CA, *et al*: CHK1-targeted therapy to deplete DNA replication-stressed, p53-deficient, hyperdiploid colorectal cancer stem cells. *Gut* 67: 903-917, 2018.
49. Altschul SF, Gish W, Miller W, Myers EW and Lipman DJ: Basic local alignment search tool. *J Mol Biol* 215: 403-410, 1990.
50. Livak KJ and Schmittgen TD: Analysis of relative gene expression data using real-time quantitative PCR and the 2^{(-delta delta C(T))} method. *Methods* 25: 402-408, 2001.
51. Contadini C, Monteonofrio L, Virdia I, Prodosmo A, Valente D, Chessa L, Musio A, Fava LL, Rinaldo C, Di Rocco G and Soddu S: p53 mitotic centrosome localization preserves centrosome integrity and works as sensor for the mitotic surveillance pathway. *Cell Death Dis* 10: 850, 2019.
52. Hothorn T and Lausen B: On the exact distribution of maximally selected rank statistics. *Comput Stat Data Anal* 43: 121-137, 2003.
53. Zhou L, Feng Y, Jin Y, Liu X, Sui H, Chai N, Chen X, Liu N, Ji Q, Wang Y and Li Q: Verbascoside promotes apoptosis by regulating HIPK2-p53 signaling in human colorectal cancer. *BMC Cancer* 14: 747, 2014.
54. Vousden KH and Prives C: Blinded by the light: The growing complexity of p53. *Cell* 137: 413-431, 2009.
55. Muller PA and Vousden KH: Mutant p53 in cancer: New functions and therapeutic opportunities. *Cancer Cell* 25: 304-317, 2014.
56. Kukcinaviciute E, Jonusiene V, Sasnauskiene A, Dabkeviciene D, Eidenaitė E and Laurinavicius A: Significance of Notch and Wnt signaling for chemoresistance of colorectal cancer cells HCT116. *J Cell Biochem* 119: 5913-5920, 2018.
57. Sadeghi MR, Jeddi F, Soozangar N, Somi MH and Samadi N: The role of Nrf2-Keap1 axis in colorectal cancer, progression, and chemoresistance. *Tumour Biol* 39: 1010428317705510, 2017.
58. Rojo de la Vega M, Chapman E and Zhang DD: NRF2 and the hallmarks of cancer. *Cancer Cell* 34: 21-43, 2018.
59. Feng Y, Zhou L, Sun X and Li Q: Homeodomain-interacting protein kinase 2 (HIPK2): A promising target for anti-cancer therapies. *Oncotarget* 8: 20452-20461, 2017.
60. Calzado MA, Renner F, Roscic A and Schmitz ML: HIPK2: A versatile switchboard regulating the transcription machinery and cell death. *Cell Cycle* 6: 139-143, 2007.
61. Kandath C, McLellan MD, Vandin F, Ye K, Niu B, Lu C, Xie M, Zhang Q, McMichael JF, Wyczalkowski MA, *et al*: Mutational landscape and significance across 12 major cancer types. *Nature* 502: 333-339, 2013.
62. Huang Y, Liu N, Liu J, Liu Y, Zhang C, Long S, Luo G, Zhang L and Zhang Y: Mutant p53 drives cancer chemotherapy resistance due to loss of function on activating transcription of PUMA. *Cell Cycle* 18: 3442-3455, 2019.
63. No JH, Kim YB and Song YS: Targeting nrf2 signaling to combat chemoresistance. *J Cancer Prev* 19: 111-117, 2014.
64. Evans JP, Winiarski BK, Sutton PA, Jones RP, Ressel L, Duckworth CA, Pritchard DM, Lin ZX, Fretwell VL, Tweedle EM, *et al*: The Nrf2 inhibitor brusatol is a potent anti-tumor agent in an orthotopic mouse model of colorectal cancer. *Oncotarget* 9: 27104-27116, 2018.